Liquid Crystals
Publication details, including instructions for authors and subscription information:
http://www.informaworld.com/smpp/title~content=t713926090

Reentrant isotropic phase in a discotic liquid crystal mixture

Wah Keat Lee[a]; Barry A. Wintner[a]; Ernest Fontes[a]; Paul A. Heiney[a]; Masashi Ohba[bc]; John N. Haseltine[b]; Amos B. Smith[b]
[a] Department of Physics and Laboratory for Research on the Structure of Matter, University of Pennsylvania, Philadelphia, Pennsylvania, U. S. A. [b] Department of Chemistry and Laboratory for Research on the Structure of Matter, University of Pennsylvania, Philadelphia, Pennsylvania, U. S. A. [c] Faculty of Pharmaceutical Science, Kanazawa University, Kanazawa, Japan

To cite this Article Lee, Wah Keat , Wintner, Barry A. , Fontes, Ernest , Heiney, Paul A. , Ohba, Masashi , Haseltine, John N. and Smith, Amos B.(1989) 'Reentrant isotropic phase in a discotic liquid crystal mixture', Liquid Crystals, 4: 1, 87 — 102

To link to this Article: DOI: 10.1080/02678298908028961

URL: http://dx.doi.org/10.1080/02678298908028961

LIQUID CRYSTALS, 1989, VOL. 4, NO. 1, 87–102

Reentrant isotropic phase in a discotic liquid crystal mixture

by WAH KEAT LEE, BARRY A. WINTNER, ERNEST FONTES
and PAUL A. HEINEY

Department of Physics and Laboratory for Research on the Structure of Matter,
University of Pennsylvania, Philadelphia, Pennsylvania 19104, U.S.A.

and MASASHI OHBA,† JOHN N. HASELTINE and AMOS B. SMITH, III

Department of Chemistry and Laboratory for Research on the Structure of
Matter, University of Pennsylvania, Philadelphia, Pennsylvania 19104, U.S.A.

(*Received 9 May 1988; accepted 12 June 1988*)

We have used X-ray diffraction and optical microscopy to study binary mixtures of 2,3,7,8,12,13-hexa-*n*-tetradecanoyloxy- and 2,3,7,8,12,13-hexa(4-*n*-undecyloxybenzoyloxy) truxenes. Our measurements confirm the existence of a reentrant isotropic phase, which is however always preceded by a mixed phase region rather than by a pure columnar phase. The nematic N_D phase displays an anomalously negative thermal expansion coefficient. We speculate on mechanisms for reentrancy in discotic mesogens.

1. Introduction

A number of condensed matter systems exhibit a phenomenon known as reentrancy, in which a disordered phase is thermodynamically stable both at high temperatures and also at temperatures below those characteristic of a more ordered phase. Examples include the melting of He^3 under pressure [1], the low-temperature normal state of superconductors containing magnetic impurities [2–4], and the phase separation of binary liquid mixtures [5]. Reentrancy has also been observed in a number of thermotropic rod-like liquid crystals [6] with the orientationally ordered but positionally disordered nematic phase appearing at both higher and lower temperatures than the layered smectic phase. At least one polar rod-like mesogen, DB_9ONO_2, exhibits a *doubly* reentrant nematic phase [7–9].

One would normally expect that the free energy, $F = U - TS$, would be minimized for the more disordered phase only at higher temperatures. Reentrancy implies that the total energy U or the entropy S of at least one of the phases must have non-negligible temperature dependence. Such a temperature dependence is often driven by competing interactions or order parameters. For example, in the case of the superconductors discussed above, the increasing tendency toward magnetic ordering at low temperature eventually makes the superconducting phase unstable. Nematic reentrancy has been phenomenologically explained [10] by a Landau theory incorporating an optimum density for the smectic phase. Recent theories [11] have suggested that the unusual smectic polymorphism observed in DB_9ONO_2 and similar mesogens is the result of frustration arising from two preferred length scales. In this case, two

---

† Present address: Faculty of Pharmaceutical Science, Kanazawa University, Takara-Machi, Kanazawa, Japan.

lengths are simultaneously present at the molecular level: the steric length of the molecule l, and a favoured dipole–dipole nearest neighbour pair length $l'(l \leqslant l' \leqslant 2l)$. In an alternate approach [12], the frustration is considered to arise primarily from the interdigitation of the molecular tails: correlated triplets of molecules propagate smectic order while dipole pairings frustrate smectic order and favor the nematic phase. Dowell [13] has emphasized the importance of tail flexibility in both stabilizing smectic phases and driving reentrant nematic and isotropic phases in rod-like liquid crystals.

Discotic liquid crystals [14] comprise a relatively new class of mesogens which are approximately disc-shaped, and which therefore tend to order in columns rather than in smectic sheets. Reentrant and inverted nematic-columnar phase sequences have been observed [15, 16] in discotic liquid crystals, although there has been little theoretical work on discotic nematic reentrancy. A possible mechanism might reside in the frustration inherent in interdigitating a hexagonal array of columns [17]. Indeed, this frustration may be linked to the incommensurate helical structure recently observed in hexaalkylthio triphenylene [19] (figure 1). de Gennes has suggested [18] that columnar order may in some cases be disrupted by pinched regions, originating from incompatible core-core and tail-tail spacings. Another unexplained feature of some discotic mesogens is the reentrant *isotropic* phase observed by Destrade *et al.* [20] (figure 2) in mixtures of 2,3,7,8,12,13-hexa(*n*-tetradecanoyloxy)- and 2,3,7,8,12,13-hexa(4-*n*-dodecyloxybenzoyloxy)-truxenes C_{13}COOTX, **5a**, and C_{12}OHBTX, **5b**. (A reentrant isotropic phase has also recently been observed [21] in a *pure* truxene derivative; low temperature non-equilibrium isotropic phases are additionally observed in discotic copper complexes [22].) To verify the Destrade *et al.* observation and to explore further the issues involved in nematic and isotropic reentrancy, we have carried out a detailed study of **5a** and a homologue of **5b** with one fewer carbon atom per chain, C_{11}OHBTX, (**5c**), using both optical microscopy and X-ray diffraction.

2. Synthesis

Truxenes **5a**, **5b**, and **5c** were synthesized according to the method of Destrade *et al.* [15] (figure 3). Specifically, the core was assembled by simple heating of commercially available 5,6-dimethoxy-1-indanone (**1**) [25] with the dehydrating agent polyphosphate ester (PPE) [23]. Hexamethoxytruxene (**2**), the major product of this process, was easily isolable by virtue of its extreme insolubility *vis-à-vis* **3**, the only significant side-product of the reaction. Demethylation of **2** proceeded readily upon exposure to boron tribromide-dimethyl sulfide complex [24]. Attachment of the radial non-polar chains was then achieved by peracylation of the derived hexahydroxy-truxene (**4**) with the appropriate acid chloride. Myristoyl chloride, used in the preparation of **5a**, is commercially available [25], while *p*-dodecyloxybenzoyl chloride [26] and *p*-undecyloxybenzoylchloride [26] were obtained from the corresponding acids [25, 26] upon treatment with thionyl chloride. The detailed experimental procedure as well as characterization data for each intermediate follow.

10,15-Dihydro-2,3,7,8,12,13-hexamethyoxy-5H-diindeno[1,2-a : 1′,2′-c]fluorene (2,3,7,8,12,13-hexamethyoxytruxene) (2). A mixture of 5,6-dimethoxy-1-indanone [25] (**1**) (5·77 g, 30 mmol) and PPE (50 ml) was heated at 130°C under Ar with stirring for 5 hours. After cooling, the reaction mixture was diluted with a mixture of chloroform (100 ml) and EtOH (20 ml) and filtered. The resulting solid was then

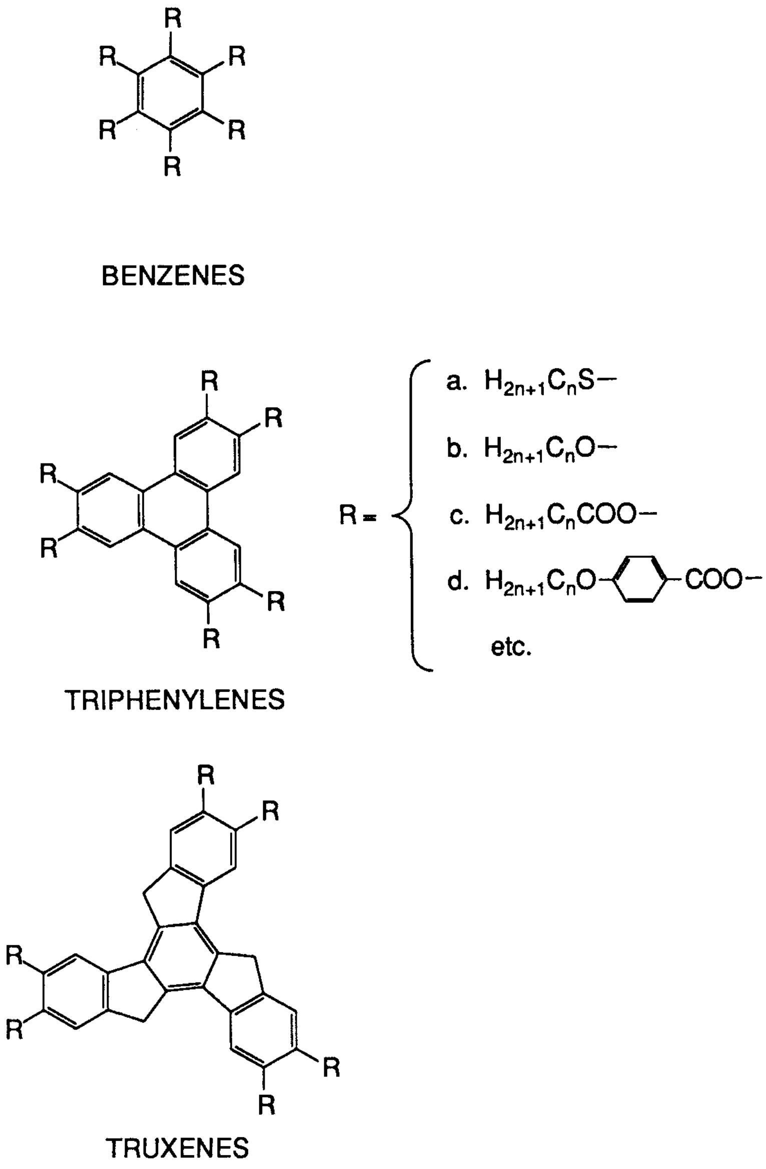

Figure 1. The benzene, triphenylene, and truxene cores, and some typical aklylated tails: (*a*) alkylthio-, (b) alkoxy-, (c) alkanoyloxy- or alkoyloxy-, (d) *p*-alkoxy-benzoyloxy-.

heated at reflux in a mixture of chloroform (50 ml) and EtOH (2 ml) for 10 min. The resulting suspension was cooled and filtered to give 3·44 g (66 per cent) of **2** as a reddish solid: mp 228°C (dec.). The first filtrate was evaporated *in vacuo* and the residue was heated at reflux in EtOH (50 ml) for 10 min. After cooling, the suspension was filtered to yield 1·52 g (28 per cent) of **3** as a yellow-brown solid: mp 221–223°C.

2. I.R. (KBr pellet) 2938 (m), 2835 (m), 1487 (s), 1462 (2), 1377 (s), 1292 (s), 1206 (s), 1189 (s), 1096 (s), 836 (m) cm^{-1}; 250 MHz ^1H N.M.R. ($CDCl_3$) δ 7·43 (s, 3H), 7·37 (s, 3H), 4·17 (s, 6H), 4·07 (s, 9H), 3·99 (s, 9H); chemical ionization mass spectrum, m/e 523·215 (M + H, calcd for $C_{33}H_{31}O_6$, 523·212).

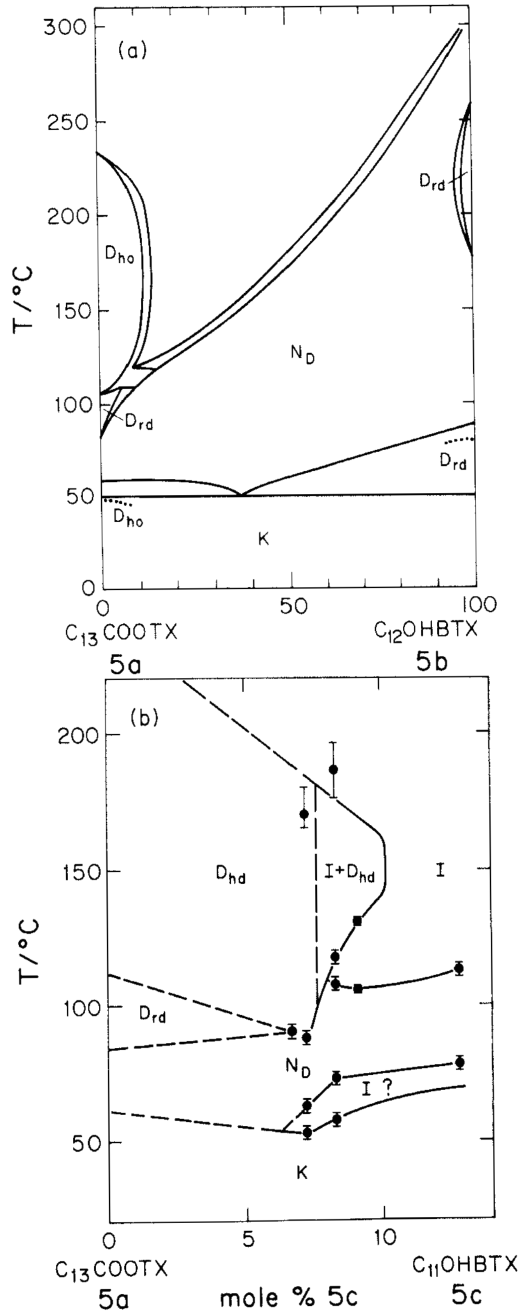

Figure 2. (*a*) Binary isobaric phase diagram for mixtures of **5a** and **5b**, from [20]. I, N_D, K, and D denote isotropic, nematic, crystalline, and columnar phases, as discussed in text. (*b*) Phase diagram for mixtures of **5a** and **5c** in the region addressed by our experiment. Points with error bars indicate transition temperatures, which were measured on heating. Solid lines are interpolated estimates of phase boundaries; dashed lines indicate phase boundaries which were not directly measured in this experiment.

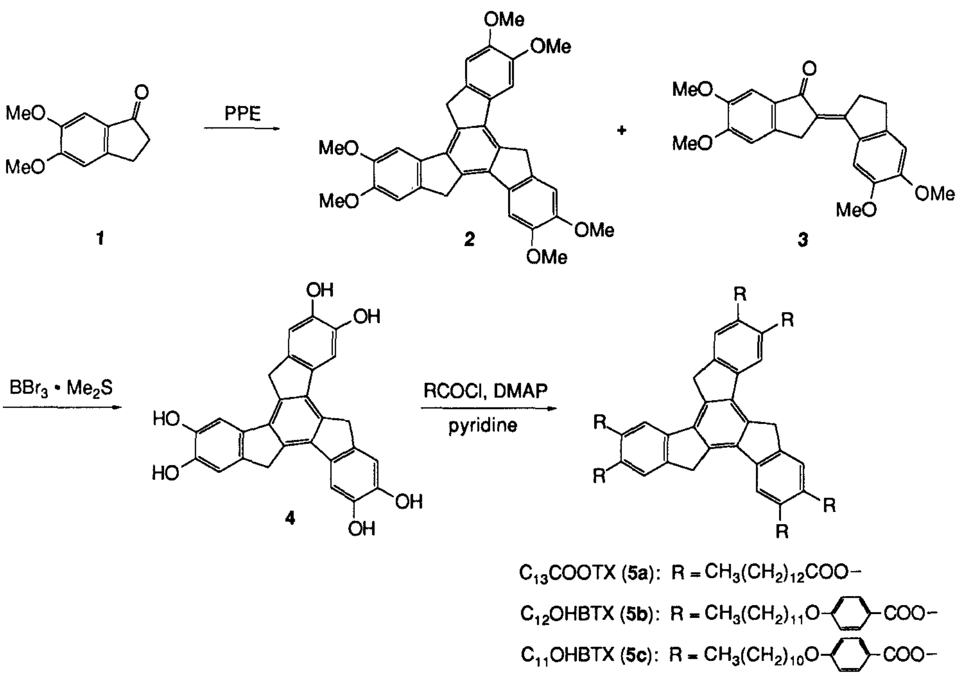

Figure 3. Synthesis of **5a**, **5b**, and **5c**.

3. I.R. ($CHCl_3$) 3011 (m), 1665 (m), 1599 (s), 1525 (s), 1498 (s), 1473 (s), 1303 (s), 1282 (s), 1252 (s), 1095 (m), 1018 (m), 845 (m) cm^{-1}; 250 MHz ^1H N.M.R. ($CDCl_3$) δ 7·28 (s, 1H), 7·26 (s, 1H), 6·99 (s, 1H), 6·90 (s, 1H), 3·98 (s, 6H), 3·93 (s, 8H), 3·56 (m, 2H), 3·07 (t, J = 5·7 Hz, 2H); chemical ionization mass spectrum, m/e 367·156 (M + H, calcd for $C_{22}H_{23}O_5$, 367·155).

10,15-Dihydro-2,3,7,8,12,13-hexahydroxy-5H-diindeno[1,2-a : 1′,2′-c]fluorene (2,3,7,8,12,13-hexahydroxytruxene) (**4**). To a suspension of **2** (4·18 g, 8·0 mmol) in 350 ml of 1,2-dichloroethane was added boron tribromide-methyl sulphide complex (30·0 g, 96 mmol) and the mixture heated at reflux under Ar with stirring for 72 hours. After cooling, H_2O (200 ml) was added and the reaction mixture extracted with ethyl acetate-EtOH (20 : 1). The extracts were washed with brine and dried ($MgSO_4$). Removal of the solvent *in vacuo* afforded a brown solid, which was heated at reflux in EtOH (30 ml) for 5 min. The suspension was cooled and filtered to give 3·02 g (86 per cent) of **4** as a brown solid: mp > 300°C; I.R. (Nujol) 3600-3100 (w, br), 2910 (m), 1598 (m), 1463 (s), 1376 (s), 1303, (s), 847 (m) cm^{-1}; 250 MHz ^1H N.M.R. (pyridine-d_5), 7·87 (s, 3H), 7·59 (s, 3H), 4·03 (s, 6H); chemical ionization mass spectrum, m/e 439·110 (M + H calcd for $C_{27}H_{19}O_6$, 439·118).

Truxene 5a. A mixture of **3** (219 mg, 0·5 mmol), tetradecanoyl chloride [25] (889 mg, 3·6 mmol), 4-dimethylaminopyridine (20 mg) and pyridine (15 ml) was stirred at room temperature for 48 hours and poured into 10 per cent aqueous HCl (80 ml). The mixture was extracted with methylene chloride and the extracts were washed successively with H_2O, saturated aqueous $NaHCO_3$, and brine, and then dried ($MgSO_4$). Removal of the solvent *in vacuo* afforded an orange solid, which was recrystallized from chloroform-EtOH (1 : 2) to give 731 mg (86 per cent) of **5a** as a slightly yellow solid. Further recrystallization of the solid from chloroform-EtOH (1 : 2) provided an analytical sample: mp (K → D_{ho}) 58–62°C; IR ($CHCl_3$) 2925 (s), 2853 (s), 1764 (s), 1478 (m), 1156 (m), 1136 (m), 1107 (m) cm^{-1}; U.V. (Et_2O) λ 305·5 nm (log ε 4·66), 296 nm (log ε 4·60), 276 nm (log ε 4·78); 250 MHz N.M.R. ($CDCl_3$), δ 7·43 (s, 3H), 7·34 (s, 3H), 3·71 (br s, 6H), 2·75–2·55 (m, 12H), 1·95–1·75 (m, 12H), 1·6–1·1 (m, 120H), 0·89 (*t*, J = 6·5 Hz, 18H).

Anal calcd. for $C_{111}H_{174}O_{12}$: C, 78·40; H, 10·31. Found: C, 78·41; H, 10·23.

Truxene 5b. A mixture of **4** (1·53 g, 3·5 mmol), 4-dimethylaminopyridine (140 mg), 4-(dodecyloxy) benzoyl chloride (8·19 g, 25·2 mmol), and pyridine 85 ml) was stirred at room temperature. After 24 h, the reaction mixture was poured into 10 per cent aqueous HCl (450 ml) and extracted with methylene chloride (2 × 100 ml). The extracts were washed successively with H_2O, saturated aqueous $NaHCO_3$, and brine, dried ($MgSO_4$), and evaporated *in vacuo* to give a dark brown oil which was crystallized from $CHCl_3$–EtOH (1 : 2) to yield 5·30 g (70 per cent) of **5b** as a yellow solid. Two recrystallizations from benzene-ethanol (1 : 1) provided an analytical sample: mp (K → N_D) 71 – 75°C; I.R. ($CHCl_3$) 2934 (s), 2857 (s), 1735 (s), 1607 (s), 1508 (s), 1475 (s), 1255 (s), 1170 (s), 1068 (s), 843 (m) cm^{-1}; U.V. (Et_2O) λ_{max} 307 nm (log ε 4·84), 274 nm (log ε 5·16), 268 m (log ε 5·17), 258 nm (log ε 5·20); 250 MHz N.M.R. ($CDCl_3$), δ 7·99 (d, J = 8·7 Hz, 6H), 7·22 (d, J = 8·2 Hz, 6H), 7·65 (br s, 6H), 6·69 (d, J = 9·0 Hz, 6H), 6·63 (d, J = 9·0 Hz, 6H), 3·95–3·75 (m, 12H), 3·65 (br s, 6H), 1·95–1·75 (m, 12H), 1·50–1·15 (m, 108H), 0·90 (t, J = 6·4 Hz, 18H).

Anal. calcd. for $C_{141}H_{186}O_{18}$: C, 78·08; H, 8·64. Found: C, 78·32; H, 8·46.

Truxene 5c. A mixture of **4** (2·19 g, 5·0 mmol), 4-dimethylaminopyridine (200 mg), 4-(undecyloxy)benzoyl chloride (11·2 g, 36·0 mmol) and pyridine (125 ml) was stirred at room temperature. After 24 hours, the reaction mixture was poured into 10 per cent aqueous HCl (600 ml) and extracted with methylene chloride. The extracts were washed successively with H_2O, saturated aqueous $NaHCO_3$, and brine, dried ($MgSO_4$), and evaporated *in vacuo* to obtain a brown gummy material, which was crystallized from benzene-EtOH (1 : 2) to yield 7·85 g (75 per cent) of **5c** as a yellow solid. Recrystallization of the solid from benzene-EtOH (1 : 1) provided an analytical sample: mp (K → D_{rd}) 87·5–91°C; I.R. ($CHCl_3$) 2922 (s), 2845 (s), 1732 (s), 1605 (s), 1510 (s), 1476 (s), 1253 (s), 1169 (s), 1067 (s), 842 (m) cm^{-1}; U.V. (Et_2O) λ_{max} 307 nm (log ε 4·86), 274 nm (log ε 5·18), 268 nm (sh. log ε 5·19), 259 nm (log ε 5·21); 250 MHz N.M.R. ($CDCl_3$), δ 7·98 and 7·81 (d each, J = 9 Hz, 12H), 7·64 (s, 6H), 6·68 and 6·63 (d each, J = 9 Hz, 12H), 3·92 and 3·81 (t each, J = 6·5 Hz, 12H), 3·65 (br s, 6H), 1·85–1·65 (m, 12H), 1·5–1·15 (m, 96H), 0·89 (t, J = 6·5 Hz, 12H).

Anal. calcd. for $C_{135}H_{174}O_{18}$: C, 77·77; H, 8·41. Found: C, 77·72, H, 8·29.

Mixtures of **5a** and **5c** with compositions from 6·7 mol % to 12·8 mol % of **5c** were studied. Typically, quantities on the order of 10 mg of **5c** and 90 mg of **5a** were weighed to a precision of 0·05 mg in powder form, and then dissolved in methylene chloride. After careful mixing, the methylene chloride was evaporated by warming to 50°C for 10–12 hours.

3. Physical measurements

For optical microscopy, a small amount of each mixture was placed between a glass slide and a cover slip, and observed with a polarizing microscope equipped with a Mettler FP5 heating and cooling stage. For the X-ray measurements, the mixtures were loaded at about 100°C into capillary tubes, which had an outer diameter of 2 mm and walls 10 μ thick. (A single-strand geometry [27] was not suitable because such strands are only stable, if at all, in columnar or crystalline phases.) Usually, about 30 mg of material were used per capillary tube. The tube were then sealed in air and placed in a temperature-controlled oven [9]. We observed a hysteresis of about 5°C in the transition temperatures; it is not clear whether this effect was intrinsic or whether it was due to wall pinning or other effects. Due to the relatively poor conductivity of the capillary tubes, the absolute temperatures of the samples are reliable only to about 3°C, but relative temperatures are accurate to better than 0·5°C. The phase transition temperatures reported here were recorded on warming. The samples tended to degrade with time at temperatures above 135°C, changing in color from yellowish orange to brownish. Degraded samples sometimes did not show the same phases on cooling from high temperatures that were seen during initial warming. For example, the 9·83 per cent mixture did not show a columnar phase after cycling in temperature twice. This may have been partly due to oxidation, since the samples were sealed in air. However, we have also observed [9] degradation in polar liquid crystals in *inert* atmosphere at temperatures above 150°C.

The X-ray diffraction measurements were done in a triple-axis configuration, similar to that described previously [9]. We used a focusing LiF (200) monochromator with a flat LiF (200) analyser and the CuK_α radiation produced by a rotating anode X-ray generator. The spot size at the sample was about 400 μ in diameter. Using the nomenclature of [9], the longitudinal and vertical resolutions of this configuration were, respectively, $\Delta q_\parallel = 0{\cdot}0045\,\text{Å}^{-1}$ full-width at half-maximum (FWHM) and $\Delta q_{vert} = 0{\cdot}26\,\text{Å}^{-1}$ FWHM; the transverse resolution $\Delta q_\perp$, which couples to the intrinsic scattering in the same way as Δq_{vert}, was much sharper than $\Delta q_\parallel$. The relatively poor vertical resolution was a consequence of the focusing geometry. In the ordered $\mathrm{D_{hd}}$ phase, discussed in more detail below, the sample texture tended to consist of a relatively small number of small 'crystallites', rather than being a 'perfect powder'. This lumpy texture, combined with the wide vertical resolution, resulted in additional structure on the low-q side of sharp peaks, and also meant that integrated peak intensities could not be reliably determined. However, we were still able to reliably measure peak positions and peak widths. The X-ray data were analysed by fitting the profiles to a lorentzian or a sum of two lorentzians, plus constant and linear background terms.

4. Results

The phase sequences originally reported by Destrade *et al.* [20] for **5a**, **5b**, and **5c** are:

5a ($\mathrm{C_{13}COOTX}$):

$$\begin{tikzcd}
\mathrm{K} \arrow[r, "90"'] \arrow[dr, shift left, "56"] & \mathrm{N_D} \arrow[r, leftrightarrow, "84"'] & \mathrm{D_{rd}} \arrow[r, leftrightarrow, "112"'] & \mathrm{D_{ho}} \arrow[r, leftrightarrow, "241"'] & \mathrm{I}, \\
& \mathrm{D_{ho}} \arrow[ul, shift left] & & &
\end{tikzcd}$$

5b ($\mathrm{C_{12}OHBTX}$):

$$\mathrm{K} \xrightarrow[90]{} \mathrm{D_{rd}} \xleftrightarrow[[79]]{} \mathrm{N_D} \xleftrightarrow[173]{} \mathrm{D_{rd}} \xleftrightarrow[260]{} \mathrm{N_D} \xleftrightarrow[>297]{} \mathrm{I},$$

5c ($\mathrm{C_{11}OHBTX}$):

$$\mathrm{K} \xrightarrow[90]{} \mathrm{D_{rd}} \xleftrightarrow[137]{} \mathrm{N_D} \xleftrightarrow[179]{} \mathrm{D_{rd}} \xleftrightarrow[284]{} \mathrm{N_D} \xleftrightarrow[297]{} \mathrm{I}.$$

Here K is a crystalline phase, N_D is the nematic phase, I is an isotropic phase, and D is a columnar discotic phase. Careful measurements of single-orientation strands [27] of **5a**, which are consistent with the present measurements, have shown that the columnar phase should be classified as D_{hd} ('hexagonal disordered') rather than D_{ho} ('hexagonal ordered'). The molecules are packed into columns which in turn form a hexagonal array with long range order. Any rectangular distortion, if it exists, must be very small. Within the columns, the molecules form a one dimensional fluid, and there is little or no column-column correlation of the molecular positions within the columns.

In figure 2 (*a*) we recall the phase diagram of Destrade *et al.* [20] for mixtures of **5a** and **5b**, while figure 2 (*b*) indicates the section of the phase diagram of **5a** and **5c** that we have measured. While the temperature scales differ slightly, the qualitative features of the two figures are the same. For mixtures in the range of 8·3 to 9·8 mol % **5c**, we see the following phase sequence on warming and cooling:

$$K \leftrightarrow I? \leftrightarrow N_D \leftrightarrow I \leftrightarrow I + D \leftrightarrow I.$$

Figure 4 shows a typical set of X-ray diffraction profiles, at a concentration of 9·83 per cent **5c**. In all phases, we see maxima in the scattering intensity near 0·22 Å^{-1} ('low-q peak') and 1·35 Å^{-1} ('high-q peak'). Measurements on single-orientation strands [27] of **5a** show two distinct high-q peaks, which can be ascribed to different mean core-core and tail–tail distances. However, the integrated intensity of the

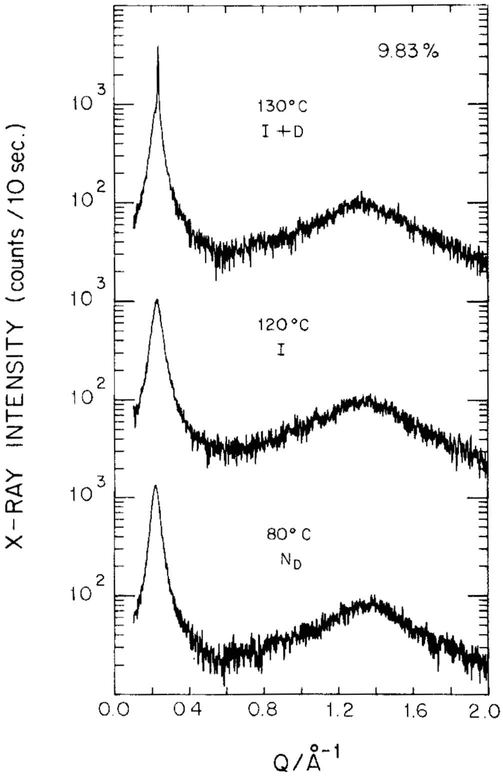

Figure 4. Complete powder X-ray profiles from a mixture of **5a** with 9·83 mol % **5c**. Data were collected upon cooling from 137°C to 56°C. Note semilogarithmic axes.

core-core peak at 1·7 Å^{-1} is an order of magnitude smaller than that of the tail–tail peak at 1·35 Å^{-1}, and as a result the core–core peak does not appear at all in the data shown in figure 4, which were measured in a powder geometry. The diffuse high-q peak we observe is therefore almost completely due to tail–tail correlations, and gives little information about intra-column core–core correlations. This peak is almost unchanged from phase to phase and in different concentrations, although there is a slight tendency toward lower q (larger real-space distance) with increasing temperature.

Figure 5 shows a set of low-q X-ray diffraction profiles, at a concentration of 8·33 per cent **5c**. The qualitative difference between the ordered D phase and the disordered I and N_D phases is dramatic: The D phase exhibits one or several sharp Bragg peaks near 0·231 Å^{-1} characteristic of the hexagonal order. By contrast the I and N_D phases only display diffuse maxima in the scattering intensity. These maxima are found

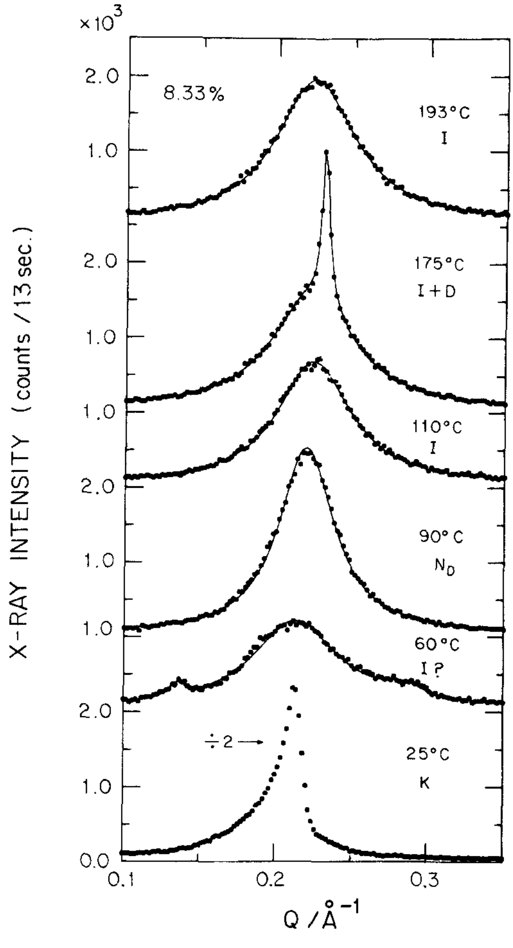

Figure 5. X-ray profiles from a mixture of **5a** with 8·33 mol % of **5c** in the range 0·10 to 0·35 Å^{-1}, at indicated temperatures. Except for the K-phase profile (bottom curve, compressed scale), which was measured at a later date on the sample, all data were measured during a heating sequence from 50°C to 197°C. Solid lines are the results of least-squares fits to lorentzian lineshapes plus linear and constant background. The asymmetry of the 25°C peak is due to the poor vertical resolution, as discussed in the text.

at approximately the same positions as the maximum in the columnar phase. This implies that there is significant local columnar order in the I and N_D phases, with distinct inter-columnar and tail–tail distances.

The distinction between the I and N_D phases is less obvious, but becomes clear when we plot peak positions and widths against temperature (figure 6). The width of the low-q diffuse peak (corresponding to short-range hexagonal correlations) is significantly larger in the I phase than in the N_D phase, and the temperature derivative of the peak position is also quite different. The N_D–I transition is also

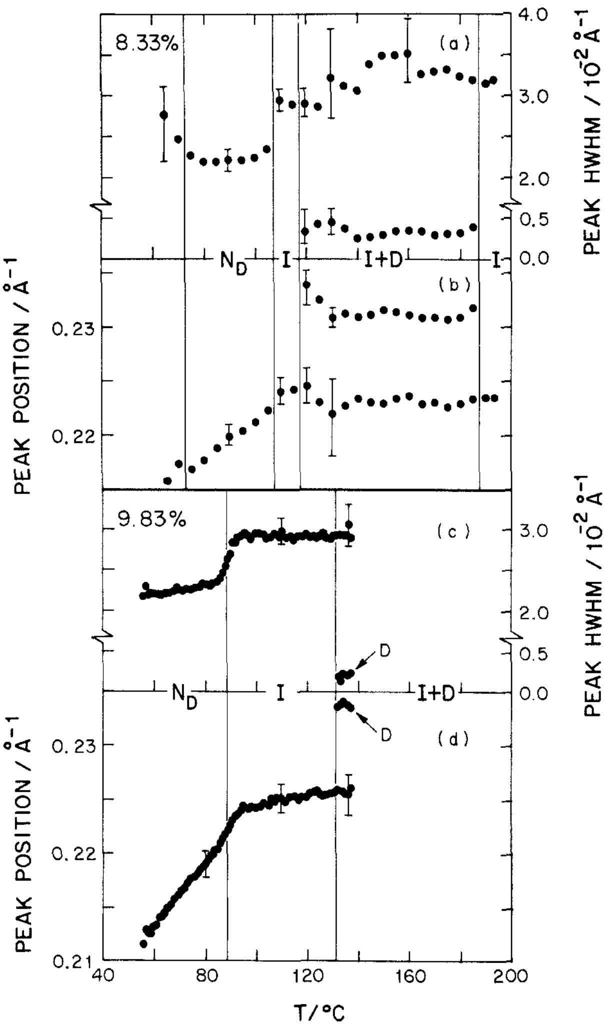

Figure 6. Fitted positions and widths of the primary hexagonal (low-q) peak from lorentzian fits to data collected on the 8·33 per cent and 9·83 per cent samples. Where more than one peak was seen, two widths and positions are given. Scatter in peak positions is primarily due to sample 'mosaic', as discussed in text. Solid bars indicate estimated systematic error due to this effect. Data on the 8·33 per cent sample were obtained by heating the sample from 50 to 197°C in 5°C increments, while data on the 9·83 per cent sample were obtained by cooling the sample from 137 to 57°C in 1°C increments. Note the breaks in the vertical scale of the peak-width plots.

easily observable under the polarizing microscope; the sample suddenly becomes dark in the I phase under cross polarizers. This reentrant I phase is similar to the high temperature I phase.

The peak positions in the isotropic phase show little or no variation with temperature. The nematic phase peak positions increase linearly with increasing temperature. This surprising result implies that the molecules move closer together as the temperature increases, i.e. that the inter-columnar thermal expansion coefficient is *negative*. A possible explanation for this effect is that the column-column distance is dominated by chain disorder. At low temperatures, the chains are more often in their fully extended, all-staggered conformation, while at higher temperatures the chains develop more kinks, thereby resulting in a shorter net column-column distance. The peak positions of the I phase suggest a nearest neighbor separation of about 28 Å, which is considerably less than the fully extended molecular dimension. The mean peak widths of the low-q peak in the N_D and I phases are 0·046 Å^{-1} and 0·058 Å^{-1} FWHM, respectively. This implies correlation lengths of $\xi = 43$ Å in the N_D phase and $\xi = 34$ Å in the I phase, corresponding to between one and two molecules.

Consistent with the phase diagram of Destrade *et al.*, upon warming the pure reentrant I phase we observe a D + I coexistence region. It is perhaps significant that we have never observed a *pure* high-temperature D phase in a mixture containing a reentrant I phase. Although it was difficult to quantify the relative fractions of the D and I phases in the coexistence region with any precision, it was generally observed that the intensity of the D-phase peaks had a maximum around 140°C. The D-phase hexagonal peaks in the coexistence region are resolution limited ($\xi > 330$ Å) and appear not to change with temperature.

Throughout the sequence of transitions discussed above, i.e. $N_D \rightarrow I \rightarrow I + D$, no significant changes were observed in the high-q (tail–tail correlation) peak. The correlation lengths associated with the high-q peak for all the samples generally varied from 3·8 to 3·3 Å, corresponding to roughly 1–2 tail-thicknesses, between $T = 80$ and $T = 130$°C. The peak positions decreased from 1·33 Å^{-1} to 1·30 Å^{-1} in the same temperature range. This means that the tails remain essentially 'melted' and that the cores never develop long range intra-column order to form a D_{ho} phase.

In three of our samples (the 12·80 per cent and 8·33 per cent and 7·20 per cent mixtures) we observed a new phase, which we have labelled 'I?', intermediate between the N_D and K phases (figure 5). This phase appears black under crossed polarizers, implying that it is optically isotropic. The X-ray signature at 60°C consists of a broad peak at 0·213 Å^{-1} with $\Delta q_{\|} \approx 0{\cdot}068$ Å^{-1} FWHM, together with weaker peaks at 0·135 Å^{-1} ($\Delta q_{\|} \approx 0{\cdot}012$ Å^{-1} FWHM) and 0·284 Å^{-1} ($\Delta q_{\|} \approx 0{\cdot}034$ Å^{-1} FWHM). The positions of these peaks agree neither with those in the D or N_D phases nor with that of the first crystalline peak, which is observed at 0·212 Å^{-1}. The correlation length calculated from the strong central peak is about 30 Å, which is slightly smaller than that observed in the higher temperature I phases. However, the satellite peaks are not consistent with a simple isotropic fluid. Upon warming to 65°C, the peak at 0·135 Å^{-1} disappears and the peak at 0·284 Å^{-1} becomes considerably weaker. The X-ray measurements at these temperatures were made only on heating, and clearly indicated the existence of a new phase. However, the optical observations were not consistently reproducible, indicating either that this phase is monotropic or that wall anchoring effects are playing a significant role.

The nature of this new phase is not understood. Since it was observed on *heating* from the crystalline phase, it is unlikely that we are observing a glass. The isotropic optical signature would tend to indicate either an isotropic liquid or a cubic condensed phase, either crystalline or liquid-crystalline. The widths of all three lines are inconsistent with crystalline long-range order, and they do not index to a simple hexagonal or cubic structure. The weak subsidiary lines are also inconsistent with a simple isotropic fluid. Nevertheless, the simplest explanations of our observations seem to be either a doubly reentrant isotropic phase with some type of positional modulation, or a disordered (liquid crystalline) phase with cubic symmetry.

5. Discussion

To address the question of mechanisms for reentrancy in discotics, it is useful to recall the systematics of reentrancy in previous measurements [28, 29]. Benzene [30] and triphenylene [31, 32] (figure 1) cores with alkyl or alkoyloxy tails have only D_h and D_r columnar mesophases, showing a typical phase sequence $K \leftrightarrow D_l \ldots D_n \leftrightarrow I$. Arguing that a bulky substituent in the alkyl tail would disrupt the columnar phase because of steric hindrance, Tinh *et al.* studied the properties of triphenylene cores with benzoate substituents [33] and found that a high temperature nematic was indeed produced; a typical phase sequence in the hexa-*p*-alkoxybenzoates of triphenylene is $K \leftrightarrow (D) \leftrightarrow N_D \leftrightarrow I$. To our knowledge, no pure benzene- or triphenylene-based mesogen shows a reentrant N_D phase.

By contrast, a truxene core with alkyl or alkoyloxy tails [15] such as **5a** yields a typical phase sequence $K \leftrightarrow (N_D) \leftrightarrow D \leftrightarrow I$; i.e. the nematic phase exists, if at all, at a lower temperature than the columnar phase. In direct analogy with the triphenylene derivatives, the hexabenzoyloxy truxenes such as **5c** develop [16], an additional high temperature nematic phase: $K \leftrightarrow N_D \leftrightarrow D \leftrightarrow N_D \leftrightarrow I$.

This brings us to the binary phase diagrams of figure 2. Truxenes **5a** and **5b** appear to be relatively immiscible in both their columnar and nematic phases. The nematic–isotropic transition temperature T_{NI} is remarkably sensitive to the composition. The low and high temperature N_D phases are thermodynamically equivalent in that they are connected by continuous paths through the phase diagram. However, the existence of a high temperature N_D phase in a pure compound depends crucially on the presence of the benzoyloxy substituent in the tail, and T_{NI} drops rapidly if even a small quantity of **5a** is added. Likewise, the D_{hd} phase of **5a** and the high temperature D_{rd} phase of **5b** can each support only a few per cent of the opposite compound. For this reason, it seems likely that in the I + D coexistence region of the 8–10 per cent **5c** mixtures we measured, the relative concentrations of the two mesogens are quite different in the I and D components of the mixture. It is clear that a bulky benzoyloxy group in the tail will tend to disrupt columnar order in **5a** due to steric repulsion. The preference of the benzoyloxy derivatives for homology in the z-direction could be due in part to a phenomenon known as π-stacking [35, 36]. Increasing evidence suggests that stabilizing dipole–dipole and van der Waals interactions can result from the collateral arrangement of molecular components incorporating suitable π-electron systems. It is therefore possible that adjacent molecules of **5b** or **5c** realize such interactions between the phenyl rings in their tails, whereas **5a** cannot participate in this mode of colligation.

The cores of truxene derivatives are all approximately 15 Å in diameter and 3·6 Å thick. The fully extended tail of **5a** is about 19 Å long, while that of **5c**, including the bulky benzoyloxy substituent, is about 2 Å longer. As Levelut has remarked [34], and as demonstrated by the diffraction profiles shown in figures 4–5, on short length scales

(1–3 molecules) the N_D, D, and I phases are almost indistinguishable. Small I-phase droplets with short-range orientational columnar order develop long range order in the N_D phase and long range positional order in the D phases, but the short range order in the three phases is quite similar. Since the two compounds do not mix well in the D phase, it is tempting to suggest that there is substantial chemical short range order in the I and N_D phases, with microscopic droplets containing primarily one molecule or the other.

From this viewpoint, the concentration variation of T_{NI} can be interpreted in two ways. Normally, for two completely miscible materials one expects the melting temperature to extrapolate linearly between the melting temperatures in the two pure materials; immiscibility is reflected in a depression of the melting temperature relative to the straight-line extrapolation. From this point of view, if **5a** and **5b** were completely miscible in the N_D phase, one would expect T_{NI} to follow a straight line from 241 to 300°C. The sharp dip in the N–I phase boundary near 10 per cent **5b** might be used as evidence that **5a** and **5b** are highly immiscible in the N_D phase. On the other hand, T_{NI} versus concentration is actually very close to a straight line with **5a**-axis intercept near 100°C. This suggests that **5b** is completely miscible in the N_D phase with any mixture of **5a** and **5b** containing more than 10 per cent **5b**, and that in fact the real anomaly is the presence of a D_{hd} phase above 100°C in pure **5a**.

This leads us to suggest that nematic, and perhaps even isotropic, reentrancy in truxene-based discotics is due to a delicate balance between positional entropy of the entire molecules and conformational entropy of the tails. (Dowell [37] also has suggested that the important role of intrachain flexibility constraints in her molecular lattice model for rod-like compounds could be extended to discotics.) As discussed above, there is a strong tendency for the tails to develop more kinks at high temperatures, i.e. the entropy of an isolated molecule is *not* constant but increases with temperature. In a D_{hd} or D_{rd} phase, the cores form irregular stacks within columns, while the tails are essentially completely 'melted' (i.e. they can assume a large number of different conformations) in the intermediate regions (figure 7 (*a*)). By contrast, in a N_D phase, the cores are positionally disordered. The positional entropy of the cores is thus increased. However, a tail located next to a core can only wander in a half-plane, and consequently has *lower* entropy; a tail caught in a region between two flat cores (circled regions in figure 7 (*b*)) can assume even fewer conformations. Thus, we propose that the columnar phases, in spite of being positionally ordered, may in fact have a larger entropy than the low temperature nematic (or even the isotropic) phase, due primarily to the greater number of conformations available to the alkyl tails. At relatively low temperatures, the tails are relatively rigid, and the free energy may be minimized in the N_D phase. As the temperature is raised in the N_D phase, the tail-conformation contribution to the entropy becomes more important, leading eventually to a D phase.

Three additional arguments support this hypothesis. First, as discussed above, we have direct evidence that the tails become shorter, and therefore more disordered, with increasing temperature in the N_D phase. Second, a low-temperature N_D phase is not observed in discotic mesogens with benzene or triphenylene cores. The area of the cores in these molecules is considerably smaller, and thus the proportional reduction of tail entropy in the N_D phase is lower. Third, the truxene cores in **5c** and other benzoyloxy-containing truxenes may be forced farther apart with increasing temperature due to the steric hindrance of the benzoyloxy group and increased motion of the cores; again, tails that are found between two cores can assume more conformations

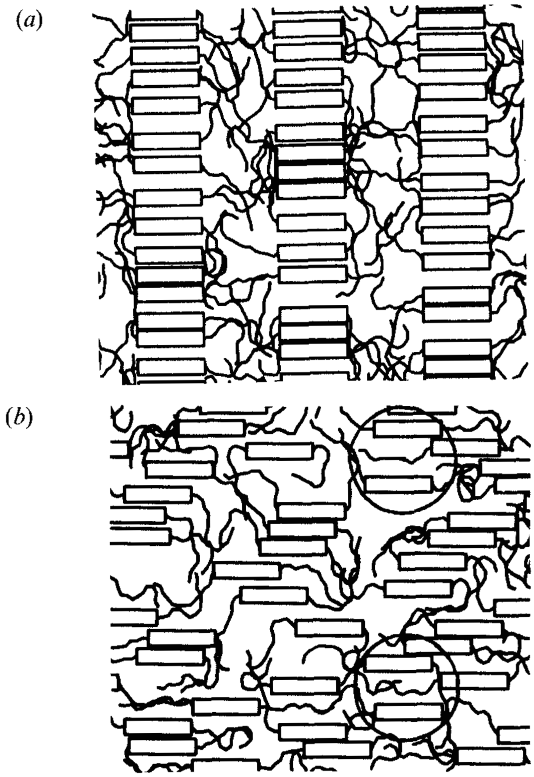

Figure 7. Schematic depictions of D and N_D phases. To produce these images, the cores were assumed to either be stacked vertically, with no tilt or transverse motion but with random height (D phase, (*a*)), or completely randomly (N_D phase, (*b*)); in either case a hard-core nearest-neighbor repulsion was included. Each tail was assumed to undergo a random walk with a minimum curvature; the motion incorporates hard-core repulsion with the cores but not with other tails. The reduction of tail entropy in the N_D phase is considered to arise as a result of configurations like the ones circled in (*b*), where a tail is trapped between two flat cores.

if the cores are relatively farther apart. This may explain the formation of a high-temperature N_D phase in these materials. (From this viewpoint, it is unfortunate that the core–core high-q peak is unobservable in our powder samples, since this third argument makes the specific prediction that the core–core separation should increase noticeably with increasing concentration of **5b** or **5c**.)

The mechanism for nematic reentrancy proposed in the previous paragraphs is largely speculative, although we think that it is quite plausible. More direct measurements on a microscopic scale, perhaps using N.M.R. or Raman spectroscopy, might prove useful in unravelling the details of tail disorder in the various phases. We also hope that our measurements will stimulate detailed theoretical calculations of the properties of these unusual materials.

The work of B. A. W. was supported by the National Science Foundation Research Experiences for Undergraduates Program, Grant PH87-12297. The work of W. K. L., E. F., and P. A. H. was supported in part by National Science Foundation Grant DMR-83-51063, and in part by support from the Research Corporation.

Acknowledgement is also made to the Donors of the Petroleum Research Fund, administered by the American Chemical Society, for the partial support of this research. The work of J. N. H., M. O., and A. B. S. was supported by the Laboratory for Research on the Structure of Matter, funded by National Science Foundation Grant DMR-8519059.

References

[1] Anderson, A. C., Reese, W., and Wheatley, J. C., 1963, *Phys. Rev.*, **130**, 1644, and references therein.

[2] Muller-Hartmann, E., and Zittarz, J., 1971, *Phys. Rev. Lett.*, **26**, 428.

[3] Riblet, G., and Winzer, K., 1971, *Solid State Commun.*, **9**, 1663.

[4] Maple, M. B., Fertig, W. A., Mota, A. C., deLong, L. E., Wohllenben, D., and Fitzgerald, R., 1972, *Solid St. Commun.*, **11**, 829. Fertig, W. A., Johnston, D. C., deLong, L. E., McCallum, R. W., Maple, M. B., and Matthias, B. T., 1977, *Phys. Rev. Lett.*, **38**, 987.

[5] Goldstein, R. E., and Walker, J. S., 1983, *J. chem. Phys.*, **78**, 1492, and references therein.

[6] Cladis, P. E., 1975, *Phys. Rev. Lett.*, **35**, 48.

[7] Tinh, Nguyen Huu, Hardouin, F., and Destrade, C., 1982, *J. Phys. Paris*, **43**, 1127.

[8] Shashidhar, R., Ratna, B. R., Surendranath, V., Raja, V. N., Krishna Prasad, S., and Nagabhusan, C., 1985, *J. Phys., Paris*, **46**, L-445.

[9] Fontes, E., Heiney, P. A., Haseltine, J. N., and Smith, A. B., III, 1986, *J. Phys., Paris*, **47**, 1533.

[10] Pershan, P. S., and Prost, J., 1979, *J. Phys., Paris*, **40**, L-27.

[11] Barois, P., Prost, J., and Lubensky, T. C., 1985, *J. Phys., Paris*, **45**, 391, and references therein.

[12] Indekeu, J. O., Berker, A. N., Chiang, C., and Garland, C. W., 1987, *Phys. Rev.* A, **35**, 1371. Indekeu, J. O., and Berker, A. N., 1986, *Physica* A, **104**, 368, and references therein.

[13] Dowell, F., 1985, *Phys. Rev.* A, **31**, 3214; 1987, *Ibid.*, **36**, 5046.

[14] For reviews, see Destrade, C., Gasparoux, H., Foucher, P., Tinh, Nguyen Huu, Malthete, J., and Jacques, J., 1983, *J. Phys. chim.*, **80**, 137. Dubois, J. C., and Billard, J., 1982, *Liq. Crystals Ordered Fluids*, **4**, 1043.

[15] Destrade, C., Malthete, J., Tinh, Nguyen Huu, and Gasparoux, H., 1980, *Physics Lett.* A, **78**, 82. Destrade, C., Gasparoux, H., Babeau, A., Tinh, Nguyen Huu, and Malthete, J., 1981, *Molec. Crystals liq. Crystals*, **68**, 37.

[16] Tinh, Nguyen Huu, Malthete, J., and Destrade, C., 1981, *J. Phys., Paris*, **42**, L-417.

[17] Prost, J., 1981, *Symmetries and Broken Symmetries*, edited by N. Boccara (IDSET).

[18] de Gennes, P. G., 1983, *J. Phys., Paris*, **44**, L-657.

[19] Fontes, E., Heiney, P. A., and de Jeu, W. H., 1988, *Phys. Rev. Lett.*, **61**, 1202.

[20] Destrade, C., Foucher, P., Malthete, J., and Tinh, Nguyen Huu, 1982, *Physics Lett.* A, **88**, 187.

[21] Warderdam, T., Frenkel, D., and Zijlstra, R. J. J., 1988, *Liq. Crystals*, **3**, 149.

[22] Ohta, K., Muroki, H., Hatada, K.-I., Yamamoto, I., and Matsuzaki, K., 1985, *Molec. Crystals liq. Crystals*, **130**, 249.

[23] Pollman, W., and Schramm, G., 1964, *Biochem. biophys. Acta*, **80**, 1.

[24] Williard, W. G., and Fryhle, C. B., 1980, *Tetrahedron Lett.*, **21**, 3731.

[25] Prepared according to the method of Gray, G. W., and Jones, B., 1953, *J. chem. Soc.*, b, 4179; *p*-dodecyloxybenzoic acid is also available from Aldrich Chemical Company, Inc., Milwaukee, Wisconsin.

[26] Arora, S. L., Fergason, J. L., and Taylor, T. R., 1970, *J. org. Chem.*, **35**, 4055.

[27] Fontes, E., Heiney, P. A., Ohba, M., Haseltine, J. N., and Smith, A. B., III, 1988, *Phys. Rev.* A, **37**, 1329.

[28] Destrade, C., Tinh, Nguyen Huu, Gasparoux, H., Malthete, J., and Levelut, A. M., 1981, *Molec. Crystals liq. Crystals*, **71**, 111.

[29] Tinh, Nguyen Huu, Malthete, J., Gasparoux, H., and Destrade, C., 1982, *Liq. Crystals Ordered Fluids*, **4**, 1123.

[30] Chandrasekhar, S., Sadashiva, B. K., and Suresh, A., 1977, *Paramana*, **9**, 471.

[31] Dubois, J. C., 1978, *Ann. Phys.*, **3**, 131.

[32] Destrade, C., Mondon-Bernaud, M., and Tinh, Nguyen Huu, 1979, *Molec. Crystals liq. Crystals Lett.*, **49**, 169.

[33] Tinh, Nguyen Huu, Destrade, C., and Gasparoux, 1979, *Physics Lett.* A, **72**, 251. Tinh, Nguyen Huu, Gasparoux, H., and Destrade, C., 1981, *Molec. Crystals liq. Crystals*, **68**, 101.

[34] Levelut, A. M., 1983, *J. Chim. phys.*, **80**, 149.

[35] Evans, D. A., Chapman, K. T., Hung, D. T., and Kawaguchi, A. T., 1987, *Agnew. Chem. Int. Ed. Engl.*, **26**, 1184.

[36] Rebek, J., Jr., Askew, B., Nemeth, D., and Parris, K., 1987, *J. Am. chem. Soc.*, **109**, 2432.

[37] Dowell, F., 1983, *Phys. Rev.* B, **28**, 3526.